Article

Synthesis and Optical Properties of Nanorattles and Multiple-Walled Nanoshells/Nanotubes Made of Metal Alloys

Yugang Sun, Benjamin Wiley, Zhi-Yuan Li, and Younan Xia

J. Am. Chem. Soc., **2004**, 126 (30), 9399-9406• DOI: 10.1021/ja048789r • Publication Date (Web): 10 July 2004

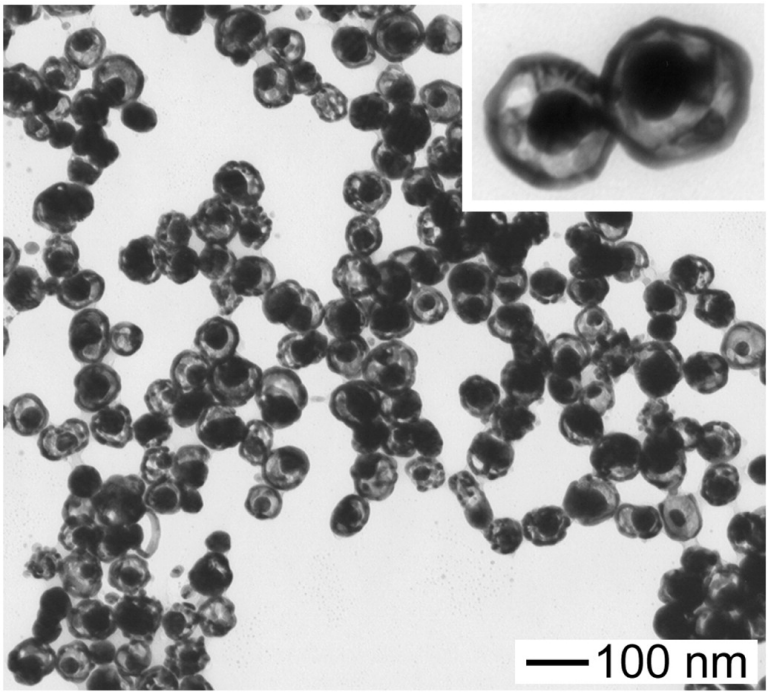

J|A|C|S
ARTICLES
Published on Web 07/10/2004

Synthesis and Optical Properties of Nanorattles and Multiple-Walled Nanoshells/Nanotubes Made of Metal Alloys

Yugang Sun,[†] Benjamin Wiley,[†] Zhi-Yuan Li,[‡] and Younan Xia*,[†]

Contribution from the Department of Chemistry, University of Washington, Seattle, Washington 98195-1700, and Laboratory of Optical Physics, Institute of Physics, Chinese Academy of Sciences, Beijing 100080, P. R. China

Received March 3, 2004; E-mail: xia@chem.washington.edu

Abstract: The galvanic replacement reaction between silver and chloroauric acid has been exploited as a powerful means for preparing metal nanostructures with hollow interiors. Here, the utility of this approach is further extended to produce complex core/shell nanostructures made of metals by combining the replacement reaction with electroless deposition of silver. We have fabricated nanorattles consisting of Au/Ag alloy cores and Au/Ag alloy shells by starting with Au/Ag alloy colloids as the initial template. We have also prepared multiple-walled nanoshells/nanotubes (or nanoscale Matrioshka) with a variety of shapes, compositions, and structures by controlling the morphology of the template and the precursor salt used in each step of the replacement reaction. There are a number of interesting optical features associated with these new core/shell metal nanostructures. For example, nanorattles made of Au/Ag alloys displayed two well-separated extinction peaks, a feature similar to that of gold or silver nanorods. The peak at ~510 nm could be attributed to the Au/Ag alloy cores, while the other peak was associated with the Au/Ag alloy shells and could be continuously tuned in the spectral range from red to near-infrared.

1. Introduction

Gold or silver nanostructures have received considerable attention for many decades because of their widespread use in applications such as catalysis, photonics, electronics, optoelectronics, information storage, chemical and biological sensing, and surface-enhanced Raman scattering (SERS) detection.[1−6] However, most studies in this area have been limited to solid nanoparticles with quasi-spherical shapes. Recent demonstrations from various research groups establish that the intrinsic properties − for example, surface plasmon resonance (or SPR), SERS, photonic, and catalytic − associated with gold or silver nanostructures can be tailored (in many cases, with a broader range of variation) by preparing these nanostructures in the core/shell configuration. For example, Au−Ag core/shell nanoparticles (with Au or Ag as the core, and Ag or Au as the shell) are characterized by two extinction peaks around 400 and 520 nm, while solid nanoparticles made of pure Ag or Au only exhibit one SPR peak.[7] In another demonstration, it has been shown that the SPR band of gold nanoshells supported on dielectric cores (e.g., silica beads or polymer latexes) could be readily swept from 500 to 1200 nm by varying their diameters and/or shell thickness.[8,9] Theoretical work has also predicted that the optical extinction peak of a gold core encapsulated in a gold shell could be greatly enhanced due to the resonance cavity

[†] University of Washington.
[‡] Chinese Academy of Sciences.

(1) Reviews: (a) Murray, C. B.; Sun, S.; Doyle, H.; Betley, T. *Mater. Res. Soc. Bull.* **2001**, *26*, 985. (b) El-Sayed, M. A. *Acc. Chem. Res.* **2001**, *34*, 257. (c) Templeton, A. C.; Wuelfing, W. P.; Murray, R. W. *Acc. Chem. Res.* **2000**, *33*, 27. (d) Halperin, W. P. *Rev. Mod. Phys.* **1986**, *58*, 533. (e) Lewis, L. N. *Chem. Rev.* **1993**, *93*, 2693.
(2) Optics and catalysis: (a) Novak, J. P.; Brousseau, L. C.; Vance, F. W.; Johnson, R. C.; Lemon, B. I.; Hupp, J. T.; Feldheim, D. L. *J. Am. Chem. Soc.* **2000**, *122*, 12029. (b) Murphy, C. J.; Jana, N. R. *Adv. Mater.* **2002**, *14*, 80. (c) Kim, F.; Song, J. H.; Yang, P. *J. Am. Chem. Soc.* **2002**, *124*, 14316. (d) Nicewarner-Peña, S. R.; Freeman, R. G.; Reiss, B. D.; He, L.; Peña, D. J.; Walton, I. D.; Cromer, R.; Keating, C. D.; Natan, M. J. *Science* **2001**, *294*, 137. (e) Ahmadi, T. S.; Wang, Z. L.; Green, T. C.; Henglein, A.; El-Sayed, M. A. *Science* **1996**, *272*, 1924. (f) Teng, X.; Black, D.; Watkins, N. J.; Gao, Y.; Yang, H. *Nano Lett.* **2003**, *3*, 261.
(3) Electronics and optoelectronics: (a) Chen, S.; Yang, Y. *J. Am. Chem. Soc.* **2002**, *124*, 5280. (b) Kamat, P. V. *J. Phys. Chem. B* **2002**, *106*, 7729. (c) Maier, S. A.; Brongersma, M. L.; Kik, P. G.; Meltzer, S.; Requicha, A. A. G.; Atwater, H. A. *Adv. Mater.* **2001**, *13*, 1501.
(4) Information storage: (a) Peyser, L. A.; Vinson, A. E.; Bartko, A. P.; Dickson, R. M. *Science* **2001**, *291*, 103. (b) Ditlbacher, H.; Krenn, J. R.; Lamprecht, B.; Leitner, A.; Aussenegg, F. R. *Opt. Lett.* **2000**, *25*, 563. (c) Link, S.; Burda, C.; Nikoobakht, B.; El-Sayed, M. A. *Chem. Phys. Lett.* **1999**, *315*, 12.
(5) Sensing and clinical diagnostics: (a) Tkachenko, A. G.; Xie, H.; Coleman, D.; Glomm, W.; Ryan, J.; Anderson, M. F.; Franzen, S.; Feldheim, D. L. *J. Am. Chem. Soc.* **2003**, *125*, 4700. (b) Roll, D.; Malicka, J.; Gryczynski, I.; Cryczynski, Z.; Lakowicz, J. R. *Anal. Chem.* **2003**, *75*, 3440. (c) Nath, N.; Chilkoti, A. *Anal. Chem.* **2002**, *74*, 504. (d) Thanh, N. T. K.; Rosenzweig, Z. *Anal. Chem.* **2002**, *74*, 1624. (e) Sun, Y.; Xia, Y. *Anal. Chem.* **2002**, *74*, 5297. (f) Kim, Y.; Johnson, R. C.; Hupp, J. T. *Nano Lett.* **2001**, *1*, 165. (g) Taton, T. A.; Mirkin, C. A.; Letsinger, R. L. *Science* **2000**, *289*, 1757.
(6) SERS: (a) Jackson, J. B.; Westcott, S. L.; Hirsch, L. R.; West, J. L.; Halas, N. J. *Appl. Phys. Lett.* **2003**, *82*, 257. (b) Dick, L. A.; McFarland, A. D.; Haynes, C. L.; Van Duyne, R. P. *J. Phys. Chem. B* **2002**, *106*, 853. (c) Cao, Y. C.; Jin, R.; Mirkin, C. A. *Science* **2002**, *297*, 1536. (d) Tessier, P. M.; Velev, O. D.; Kalambur, A. T.; Rabolt, J. F.; Lenhoff, A. M.; Kaler, E. W. *J. Am. Chem. Soc.* **2000**, *122*, 9554. (e) Nie, S.; Emory, S. R. *Science* **1997**, *275*, 1102.
(7) (a) Bohren, C. F.; Huffman, D. R. *Absorption and Scattering of Light by Small Particles*; Wiley: New York, 1983. (b) Bönnemann, H.; Hormes, J.; Kreibig, U. Nanostructured Metal Clusters and Colloids. In *Handbook of Surface and Interfaces of Materials*; Nalwa, H. S., Ed.; Academic Press: San Diego, 2001; Vol. 3, pp 1−87.
(8) (a) West, J. L.; Halas, N. J. *Annu. Rev. Biomed. Eng.* **2003**, *5*, 285. (b) Oldenburg, S. J.; Jackson, J. B.; Westcott, S. L.; Halas, N. J. *Appl. Phys. Lett.* **1999**, *75*, 2897.
(9) (a) Westcott, S. L.; Jackson, J. B.; Radloff, C.; Halas, N. J. *Phys. Rev. B* **2002**, *66*, 155431. (b) Prodan, E.; Nordlander, P. *Nano Lett.* **2003**, *3*, 543.

effect.[10] These demonstrations have triggered an enormous amount of research efforts with a specific interest on the synthesis and optical characterization of gold or silver nanostructures having a core/shell or hollow structure.

Core/shell metal nanostructures are commonly synthesized by directly depositing the metal on the surfaces of colloidal templates that can be readily synthesized using various methods. For example, a number of research groups have explored how gold or silver shells could be deposited on the surfaces of spherical colloids made of silica or organic polymers. As shown by Halas and co-workers, gold nanocrystals of 1−2 nm in size could be effectively adsorbed onto the surfaces of silica beads that had been derivatized with monolayers of 3-amino-propyltrimethoxysilane in advance. The deposited gold nanoparticles could then serve as nucleation sites for the deposition of more gold through an electroless plating process, resulting in the formation of a complete shell of gold on each silica bead.[11] The surfaces of hydroxyl-terminated silica colloids have also been activated by chemical treatment in a solution containing both $SnCl_2$ and HCl. The Sn-enriched outmost layer could promote the nucleation and deposition of gold via the reduction of $HAuCl_4$ with formaldehyde.[12] More recently, a sonochemical method has been demonstrated to deposit nanoparticles of gold (or silver) on the surfaces of silica beads to form shell-like structures.[13] In this process, a slurry of silica colloids (prepared using a modified Stöber method), $HAuCl_4$ (or $AgNO_3$), and ammonia was subjected to ultrasonic irradiation in an aqueous medium. In another demonstration, polystyrene latexes modified with a polyelectrolyte such as positively charged poly(ethylene imine) were used as sacrificial templates to build composite nanoshells (consisting of gold and the polymer) through the adsorption and self-assembly of oppositely charged gold colloids and polymer chains in a layer-by-layer scheme.[14]

Hollow shells made of metals are readily obtained by selectively removing the cores via calcination or chemical etching.[15] It is also worth pointing out that the surfaces of the gold nanoshells obtained by these methods could be coated with silica layers (by using some well-established procedures) to further modify the SPR properties.[16] By repeating the gold and silica deposition steps, Halas and co-workers have successfully prepared nanoparticles with multiply, concentric shells of gold and silica.[17] In a related study, we have also demonstrated that gold nanoparticles could be coated with double shells made of silica and polymer. After the silica shell sandwiched between the gold core and the polymer shell had been selectively removed by etching in a HF solution, rattle-like nanostructures (i.e., core/shell particles with cores movable inside the shells) have been successfully synthesized.[18] In this approach, the size of the core, the thickness of the shell, and the separation between the core and the shell could all be separately controlled by varying the experimental parameters.

We have recently demonstrated a different method based on the galvanic replacement reaction for preparing hollow nanostructures composed of metals such as Au, Pd, Pt, and their alloys.[19] Hollow nanostructures prepared using this approach are characterized by well-defined void sizes, wall thicknesses, shapes, and highly crystalline walls with controllable surface porosities.[20] In the present demonstration, we combine the replacement reaction (between Ag and $HAuCl_4$) with electroless plating of silver to further extend the capability of this method to fabricate core/shell metal nanostructures characterized by complex configurations and hybrid compositions.[21] We have concentrated on three major examples: nanorattles where Au/Ag solid nanoparticles are encapsulated within Au/Ag alloy nanoshells with or without pores in their surfaces; and multiple-walled nanoshells/nanotubes (or nanoscale Matrioshka) whose walls are composed of Au/Ag alloys and/or Pd/Ag alloys. These new types of core/shell nanostructures are expected to find use in a number of applications that may include plasmonics, SERS detection, colorimetric sensing, catalysis, and information storage.

2. Experimental Section

Chemicals and Materials. Silver nitrate ($AgNO_3$, 99+%), chloroauric acid ($HAuCl_4$, 99.9%), anhydrous ethylene glycol (EG, 99.8%), poly(vinyl pyrrolidone) (PVP, $M_w \approx 55\,000$), and L-ascorbic acid (99+%) were purchased from Aldrich (Milwaukee, WI) and used without further purification. Sodium citrate ($Na_3C_6H_5O_7$, 99.8%) and sodium chloride (NaCl, 99.9%) were obtained from Fisher Scientific (Fair Lawn, NJ). Palladium nitrate, $Pd(NO_3)_2$ (99.9%), was bought from Alfa Aesar (Ward Hill, MA). Water used in all experiments had been purified with cartridges from Millipore (E-pure, Dubuque, IA) to a resistivity of 18 MΩ cm. Copper grids (coated with carbon films) for transmission electron microscopy (TEM) studies were obtained from Ted Pella (Redding, CA). Silicon wafers used for the preparation of scanning electron microscopy (SEM) samples were ordered from Silicon Valley Microelectronics (San Jose, CA).

Synthesis of Silver Nanostructures. Silver nanostructures (including quasi-spheres, cubes, and wires) were prepared using a modified polyol process,[22] in which EG served as both solvent and reducing agent, PVP as a capping reagent and colloidal stabilizer, and $AgNO_3$ as a precursor to elemental silver. In a typical synthesis of quasi-spherical nanoparticles, 0.025 g of $AgNO_3$ and 0.10 g of PVP were dissolved in 10 mL of EG at room temperature. The solution was then heated at 160 °C in an oil bath for 1.5 h. Silver nanocubes were prepared using a procedure described in our previous report, with some minor modifications.[22a] In this case, 3 mL of EG solution of $AgNO_3$ (0.25 M, prepared at room temperature) and PVP (0.19 M in terms of the repeating unit), and 3 mL of EG solution of PVP (0.19 M, prepared at room temperature) were simultaneously added to 5 mL of hot EG (heated at 160 °C) using a two-channel syringe pump (KDS-200, Stoelting, Wood Dale, IL) at a rate of 22.5 mL/h. The mixture was continued with heating at 160 °C for 40 min. Silver nanowires were prepared using a procedure

(10) Baer, R.; Neuhauser, D.; Weiss, S. *Nano Lett.* **2004**, *4*, 85.
(11) (a) Oldenburg, S. J.; Averitt, R. D.; Westcott, S. L.; Halas, N. J. *Chem. Phys. Lett.* **1998**, *288*, 243. (b) Jackson, J. B.; Halas, N. J. *J. Phys. Chem. B* **2001**, *105*, 2743.
(12) Lim, Y. T.; Park, O. O.; Jung, H.-T. *J. Colloid Interface Sci.* **2003**, *263*, 449.
(13) Pol, V. G.; Gedanken, A.; Calderon-Moreno, J. *Chem. Mater.* **2003**, *15*, 1111.
(14) (a) Caruso, F.; Spasova, M.; Salgueiriño-Maceira, V.; Liz-Marzán, L. M. *Adv. Mater.* **2001**, *13*, 1090. (b) Ji, T.; Lirtsman, V. G.; Avny, Y.; Davidov, D. *Adv. Mater.* **2001**, *13*, 1253.
(15) (a) Yin, Y.; Lu, Y.; Gates, B.; Xia, Y. *Chem. Mater.* **2001**, *13*, 1146. (b) Zhong, Z.; Yin, Y.; Gates, B.; Xia, Y. *Adv. Mater.* **2000**, *12*, 206. (c) Ung, T.; Liz-Marzán, L. M.; Mulvaney, P. *Langmuir* **1998**, *14*, 3740. (d) Caruso, F.; Caruso, R. A.; Möhwald, H. *Science* **1998**, *282*, 1111.
(16) Stöber, W.; Fink, A.; Bohn, E. *J. Colloid Interface Sci.* **1968**, *26*, 62.
(17) Prodan, E.; Radloff, C.; Halas, N. J.; Nordlander, P. *Science* **2003**, *302*, 419.
(18) (a) Kamata, K.; Lu, Y.; Xia, Y. *J. Am. Chem. Soc.* **2003**, *125*, 2384. (b) Kim, M.; Sohn, K.; Na, H. B.; Hyeon, T. *Nano Lett.* **2002**, *2*, 1383.
(19) (a) Sun, Y.; Mayers, B.; Xia, Y. *Adv. Mater.* **2003**, *15*, 641. (b) Sun, Y.; Mayers, B. T.; Xia, Y. *Nano Lett.* **2002**, *2*, 481.
(20) (a) Sun, Y.; Xia, Y. *J. Am. Chem. Soc.* **2004**, *126*, 3892. (b) Sun, Y.; Xia, Y. *Nano Lett.* **2003**, *3*, 1569.
(21) Sun, Y.; Xia, Y. *Adv. Mater.* **2004**, *16*, 264.
(22) (a) Sun, Y.; Xia, Y. *Science* **2002**, *298*, 2176. (b) Sun, Y.; Xia, Y. *Adv. Mater.* **2002**, *14*, 833. (c) Sun, Y.; Yin, Y.; Mayers, B. T.; Herricks, T.; Xia, Y. *Chem. Mater.* **2002**, *14*, 4736. (d) Sun, Y.; Gates, B.; Mayers, B.; Xia, Y. *Nano Lett.* **2002**, *2*, 165.

similar to the one used for the synthesis of silver nanocubes, except for the difference in concentration for $AgNO_3$ and PVP.[22b] In this case, 3 mL of EG solution of $AgNO_3$ (0.085 M) and 3 mL of EG solution of PVP (0.13 M) were used.

Synthesis of Au/Ag Alloy Nanoparticles. Nanoparticles of Au/Ag alloys were prepared using the procedure described elsewhere.[23] The total concentration of $HAuCl_4$ and $AgNO_3$ was kept at 0.25 mM. In the first step of synthesis, an appropriate volume of 30 mM $HAuCl_4$ solution was diluted with 50 mL of water, and this solution was transferred into a 250-mL round-bottom flask and heated to boiling with a mantle heater. At this point, 20 mM $AgNO_3$ solution of various volumes was added to the reaction mixture. Note that the production of homogeneous Au/Ag alloys would be affected by the formation of AgCl precipitates if $AgNO_3$ solution was added to the aqueous $HAuCl_4$ solution at lower temperatures (e.g., room temperature). After 2.5 mL of 1% (by weight) sodium citrate solution had been introduced, the mixture was refluxed for another 30 min. The final solution was then allowed to cool for further characterization and next-step syntheses. Vigorous magnetic stirring was maintained throughout the synthesis. Alloyed nanoparticles with gold molar fractions in the range of 0−1.0 could be readily prepared by controlling the molar ratio between the $AgNO_3$ and $HAuCl_4$ solutions added to the reaction system.

Synthesis of Nanorattles Consisting of Au/Ag Alloy Cores and Shells. Water was used as the solvent for all galvanic replacement reactions. Here, we use the $Au_{0.75}Ag_{0.25}$ alloy colloids as a typical example to illustrate the synthetic procedure: 1 mL of a solution of ascorbic acid (100 mM) was added to a 5 mL dispersion of the as-obtained Au/Ag alloy colloids, followed by dropwise addition of 1 mL of 5 mM $AgNO_3$. The mixture was then allowed to react for 30 min at room temperature. The reaction mixture was centrifuged at 2000 rpm for 15 min to remove the excess reducing agents (e.g., ascorbic acid and sodium citrate). The final product (Au/Ag alloy colloids whose surfaces were coated with conformal shells of pure silver) were collected and redispersed in 5 mL of water. After this new dispersion had been heated to its boiling temperature, a certain aliquot (e.g., 0.4, 0.5, or 0.6 mL) of 1 mM $HAuCl_4$ solution was added dropwise and under vigorous magnetic stirring. The hot mixture was continued with refluxing for another 20 min to generate nanorattles consisting of Au/Ag alloy cores and Au/Ag alloy shells.

Preparation of Hollow Nanostructures with Multiple Walls. The synthetic procedure for Au/Ag multiple-walled nanotubes has been published.[21] In a typical synthesis of multiple-walled nanoshells, 0.25 mL of the as-obtained dispersion of silver nanoparticles was added to 5 mL of water. After refluxing for 15 min, 0.8 mL of 1 mM $HAuCl_4$ aqueous solution was introduced dropwise, and the mixture was continued with boiling for another 20 min until the color became stable. In forming layers of pure silver on these single-walled Au/Ag nanoshells, 3 mL of the as-obtained dispersion was mixed with 0.6 mL of 100 mM ascorbic acid at room temperature, followed by the introduction of 0.6 mL of 5 mM $AgNO_3$. The electroless plating was allowed to proceed for 30 min at room temperature. The product was centrifuged at 2000 rpm for 15 min to remove the excess ascorbic acid. For the synthesis of double-walled Au/Ag nanoshells, the Ag-coated nanoshells were redispersed in 5 mL of water and used for the second round of galvanic replacement reaction by reacting with 0.6 mL of 1 mM $HAuCl_4$ aqueous solution. Triple-walled Au/Ag nanoshells were synthesized by repeating the silver plating process (with 1 mL of 5 mM $AgNO_3$) and the galvanic replacement reaction (with 1 mL of 1 mM $HAuCl_4$). Cubic nanoboxes containing multiple shells and nanotubes with multiple sheaths were prepared using a similar procedure. Double-walled nanoshells with the outer shells consisting of a Pd/Ag alloy and the inner shell consisting of a Au/Ag alloy were synthesized by switching $HAuCl_4$ to $Pd(NO_3)_2$ solution (10 mM) in the second round of replacement reaction. Magnetic stirring was maintained throughout all syntheses. AgCl precipitates formed in the mixture were dissolved by saturating the reaction solution with NaCl powder. The product of each reaction was collected by centrifugation and rinsed with water for several times. The final products were redispersed in water for further characterization and usage.

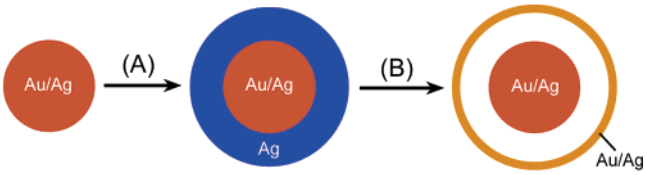

Figure 1. Schematic illustration of the procedure for preparing a nanorattle consisting of Au/Ag alloy core and Au/Ag alloy shell. Two major steps are involved: (A) electroless deposition of a conformal coating of pure silver on the surface of a Au/Ag alloy nanoparticle; and (B) reaction of the resultant particle with an aqueous $HAuCl_4$ solution to transform the coating of pure silver into a Au/Ag alloy shell larger in size. Although both the core and the shell of the nanorattle are made of Au/Ag alloys, they may differ in elemental composition, depending on the amount of $HAuCl_4$ added to the reaction system.

Instrumentation. The samples for TEM and SEM studies were prepared by placing small drops of the dispersions of metal nanostructures on carbon-stabilized copper grids and silicon substrates, respectively. The samples were then allowed to dry at room temperature in a fume hood. The TEM images and electron diffraction patterns were taken using a JEOL microscope (1200 EX II) operated at 80 kV. The SEM images were obtained using a field-emission microscope (Sirion XL, FEI, Hillsboro, OR) operated at 15 kV. Energy-dispersive X-ray (EDX) analysis was performed using an EDAX system attached to the same electron microscope. All UV−visible−near-infrared (NIR) spectra were recorded at room temperature on a Cary 5E (Varian, Walnut Creek, CA) spectrometer, with a quartz cuvette of 1 cm in optical path length.

3. Results and Discussion

Nanorattles Consisting of Au/Ag Alloy Cores and Shells. Figure 1 shows a schematic of the synthetic procedure. The first step involved the deposition of a conformal layer of pure silver on the surface of a Au/Ag alloy nanoparticle. In the past, Au@Ag core/shell nanoparticles have been prepared by directly depositing Ag on the surfaces of Au nanoparticles using a number of methods that include radiolysis − exposure of a mixture of Au colloids and $NaAg(CN)_2$ to γ-radiation,[24] and electroless plating − reduction of $AgNO_3$ with various chemical reagents at room temperature.[25] In the present approach, we directly mixed the as-obtained dispersion of Au/Ag alloy colloids with an aqueous solution containing ascorbic acid and $AgNO_3$ at room temperature. Reduction of $AgNO_3$ by ascorbic acid resulted in silver atoms, which nucleated and grew on the surfaces of Au/Ag alloy colloids. We found that the Au/Ag colloids could still be well coated with silver shells even if their molar fractions of gold were as low as 0.05. However, colloids made of pure gold could not be coated with homogeneous shells of silver, indicating that the silver atoms probably sit on the surfaces of Au/Ag alloy colloids and facilitated the reduction of $AgNO_3$, as well as the nucleation and deposition of Ag atoms at the interface. The second step involved the galvanic replacement reaction between Ag-coated Au/Ag alloy colloids (referred to as Au/Ag@Ag colloids in the following discussion) with an

(23) Sun, Y.; Xia, Y. *Analyst* **2003**, *128*, 686.

(24) (a) Henglein, A.; Meisel, D. *Langmuir* **1998**, *14*, 7392. (b) Mulvaney, P.; Giersig, M.; Henglein, A. *J. Phys. Chem.* **1993**, *97*, 7061.

(25) (a) Kim, Y.; Johnson, R. C.; Li, J.; Hupp, J. T.; Schatz, G. C. *Chem. Phys. Lett.* **2002**, *352*, 421. (b) Henglein, A.; Giersig, M. *J. Phys. Chem. B* **1999**, *103*, 9533. (c) Sinzig, J.; Radtke, U.; Quinten, M.; Kreibig, U. *Z. Phys. D* **1993**, *26*, 242.

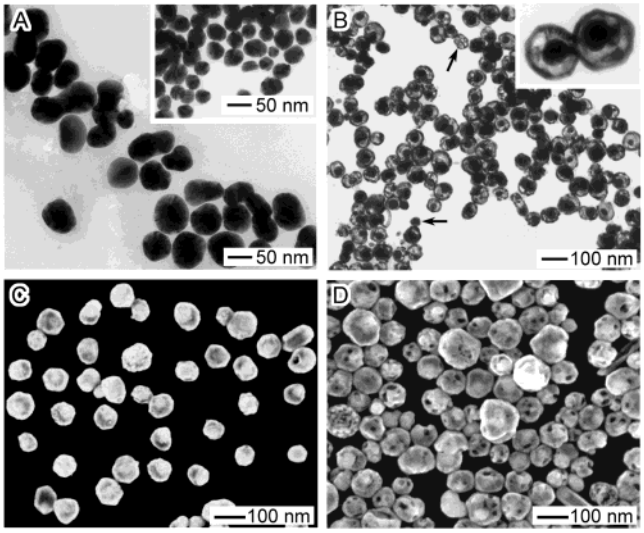

Figure 2. (A) TEM image of Au/Ag alloy colloids (with a gold mole fraction of 0.75) whose surfaces have been coated with conformal shells of pure silver. The inset shows a TEM image of the Au/Ag alloy colloids before silver coating. (B) TEM and (C) SEM images of nanorattles that were prepared by adding 0.4 mL of $HAuCl_4$ solution to the silver-coated Au/Ag colloids. The SEM image indicates that the Au/Ag shells of these nanorattles are continuous and smooth. (D) SEM image of another sample that was prepared by increasing the volume of $HAuCl_4$ solution to 0.6 mL. As a result of dealloying, the Au/Ag shells of resultant nanorattles were interspersed with small holes.

aqueous $HAuCl_4$ solution at 100 °C. The conformal coating of pure silver was transformed into a shell made of a Au/Ag alloy through the galvanic replacement process. Note that the spacing between the core and the shell is mainly determined by the thickness of the pure silver coating, which could be varied by changing the concentration of $AgNO_3$ in the electroless plating bath.

Because the inner diameter of the shell was larger than the size of the core, it was believed that the Au/Ag core encapsulated in each Au/Ag shell was potentially movable if the system was immersed in a liquid medium. This notion is partially supported by the following observation (see Figure S1 and Table S1 in the Supporting Information): When the TEM sample was prepared by holding the grid at a tilting angle of 70° relative to the horizontal direction during solvent evaporation, 40% of the cores were located at the bottom of the shells and 21% of the cores were located at the top ceilings of the shells. In comparison, when the TEM sample was prepared without any tilting, there was essentially no difference (30% versus 27%) between these two opposite locations. These results suggest that some of the cores were able to move as the solvent was being evaporated to be positioned at the most favorable locations (i.e., bottom of the shells) under the influence of gravitational field.

The nanostructures involved in each reaction step have been fully characterized using TEM and SEM. Figure 2A shows a typical TEM image of the Au/Ag alloy colloids (with a 0.75 molar fraction for Au) after their surfaces had been coated with conformal shells of pure silver. The inset gives a TEM image of the Au/Ag alloy colloids before silver coating. Both samples were quasi-spherical in shape. The mean diameter had been increased from ~30 to ~70 nm after silver coating. As the silver-coated colloids were subjected to the galvanic replacement reaction with $HAuCl_4$, the layers of pure silver were transformed into nanoshells made of a Au/Ag alloy.[20] Two typical TEM and SEM images of the product are shown in Figure 2B and C, respectively. As is clearly depicted in the inset of Figure 2B, the product was characterized by a rattle-like structure (referred to as a nanorattle), with a potentially movable core (Au/Ag solid particle) being encapsulated within a metal shell whose inner diameter was larger than the diameter of the core. Statistical analysis over several hundred particles indicates that the yield of such nanorattles could be as high as 95% in each run of synthesis. This result suggests that most of the Au/Ag colloids (Figure 2A) had been completely coated with conformal shells of pure silver even though we only employed a simple electroless plating process. As is marked by arrows, there were two major types of defects in the product: (i) Au/Ag nanoshells containing no cores that resulted from pure silver nanoparticles formed in the electroless plating process; and (ii) pure Au nanoparticles that could not be coated with silver and thus covered by no Au/Ag alloy shell. It is also possible for the cores to come out if the shells were broken. Note that most cores were not located in the centers of these nanorattles (see the statistical analysis in Table S1). This observation also led us to suspect that the encapsulated Au/Ag solid core was able to move freely inside each shell if it was filled with a liquid such as water. As the solvent was evaporated, the core tended to move close to the wall of each shell as a result of the attractive capillary force and dipole interaction between their surfaces.[26] The nanorattles shown in Figure 2B and C were prepared by reacting 5 mL of Au/Ag alloy colloids with 0.4 mL of $HAuCl_4$ solution. Their surfaces were smooth and essentially free of pinholes. When the volume of $HAuCl_4$ solution was increased to 0.6 mL, the Au/Ag shells of resulting nanorattles were interspersed with small holes due to dealloying.[20] In principle, the thickness, composition, and surface porosity of the Au/Ag alloy shells could all be tailored (but not independently due to the entanglement of replacement reaction, alloying, and dealloying processes) by controlling the thickness of pure silver coating and/or the degree of replacement between the pure Ag layer and the $HAuCl_4$ solution.

Surface Plasmon Resonance Properties of the Au/Ag Alloy Nanorattles. It is known that nanostructures made of silver or gold exhibit intense colors due to their strong SPR in the visible region. Here, we found that the UV−visible−NIR extinction spectra of the newly synthesized nanorattles were different from those of conventional solid or hollow nanoparticles. Figure 3A shows the typical spectra taken from aqueous suspensions of Au/Ag nanorattles in the spectral range of 350−1250 nm. The original Au/Ag alloy core nanoparticles (see the inset of Figure 2A for a TEM image) were also included, which exhibited only one sharp peak centered at ~502 nm (Figure 3A, curve a). This observation was in agreement with the results of previous studies.[27] When Au/Ag alloy shells with larger inner diameters were placed around the solid nanoparticles (as shown in Figure 2B), another well-resolved peak at longer wavelength was observed in addition to the peak around 510 nm. This new extinction peak was believed to originate from the SPR scattering of the Au/Ag shells.[11] To better understand the experimentally observed spectra, we also calculated the extinction coefficient (Figure 3B) of a nanorattle whose core and shell had the same elemental composition of $Au_{0.75}Ag_{0.25}$. The

(26) Korgel, B. A.; Fitzmaurice, D. *Adv. Mater.* **1998**, *10*, 661.
(27) Link, S.; Wang, Z. L.; El-Sayed, M. A. *J. Phys. Chem. B* **1999**, *103*, 3529.

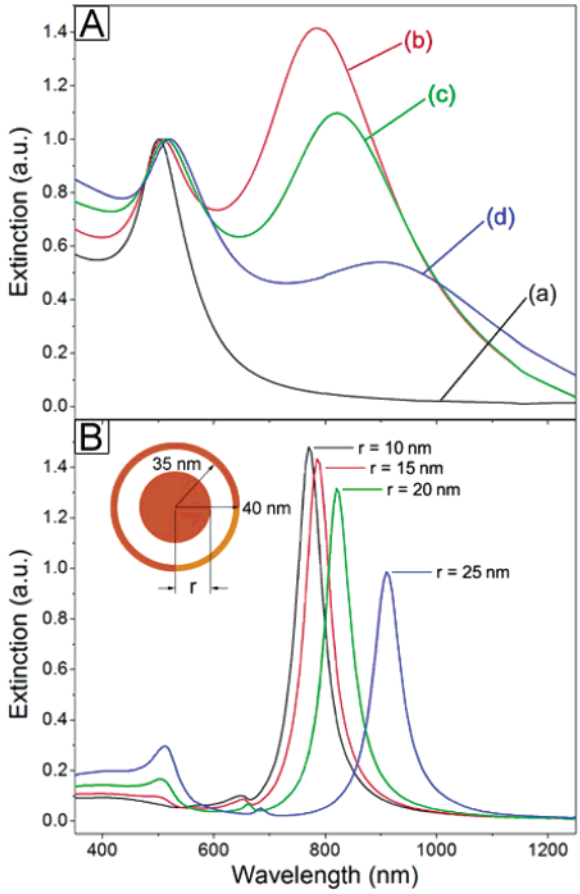

Figure 3. (A) UV−visible−NIR extinction spectra of nanorattles that were prepared by titrating the same amount of Ag-coated Au/Ag colloids with different volumes of 1 mM $HAuCl_4$ solution: (a) 0; (b) 0.4; (c) 0.5; and (d) 0.6 mL. All of the spectral curves were normalized against the intensities of peaks around 510 nm. (B) Extinction spectra calculated for a nanorattle whose core and shell contained 75% of Au and 25% of Ag. The inner and outer diameters of the shell were fixed at 70 and 80 nm, respectively. The diameter of the core was varied from 20 to 50 nm. As a result, the spacing between the core and inner surface of the shell was varied from 25 to 10 nm, respectively.

refractive index of this alloy was then calculated from the refractive indices of pure gold and silver using a linear combination. We also fixed the dimension of the nanoshell and maintained the spherical symmetry for the nanorattle by assuming that the core (with variable diameters) was located in the center of the shell. In this case, we could still use the exact solution to Mie scattering that was derived for a concentric, spherical system.[28] The results shown in Figure 3B suggest that there was no coupling between the core and shell (in other words, the core would be screened by the shell and no SPR would be excited in the core) if the core and the inner surface of the shell was separated by more than 20 nm. As the separation was reduced below 20 nm, the SPR modes of both core and shell could be excited and the spectra would display two well-separated extinction peaks. These results also indirectly support the notion that the core in the nanorattle we have synthesized is movable within the shell so the separation between the core and the inner surface of the shell can be smaller than 20 nm. In comparison, TEM images taken from dried samples showed a separation in the range of 30−40 nm. Due to Brownian motion, it is believed that the core can move around inside each shell to make its virtual physical volume much larger than its actual size determined from TEM imaging studies.

We have recently demonstrated that the SPR extinction peak of Au/Ag alloy nanoshells could be continuously tuned in the red and near-infrared regions by controlling the alloying and dealloying processes involved in the galvanic replacement reaction.[20] For the same reason, the SPR features of our nanorattles could also be tuned by reacting the Au/Ag@Ag nanoparticles with different volumes of $HAuCl_4$ solution. As the volume of 1 mM $HAuCl_4$ solution added to the same amount of Au/Ag@Ag nanoparticles was increased, the SPR peak of Au/Ag shells was significantly shifted to the red (together with some reduction in the intensity), while the SPR peak corresponding to the solid cores was slightly broadened and red-shifted. More specifically, when the same amount of Au/Ag@Ag particles was reacted with 0.4 mL of 1 mM $HAuCl_4$ solution, the product displayed a SPR peak at 784 nm (curve b, Figure 3A). This peak was greatly shifted to 903 nm (curve d, Figure 3A) when the volume of $HAuCl_4$ solution was increased to 0.6 mL. The red shift of this peak could be attributed to the decrease in wall thickness for the outer shells, as well as the generation of pinholes in the walls due to selective removal of Ag. Meanwhile, the SPR peak corresponding to the solid cores was shifted by only 14 nm (i.e., from 507 to 521 nm), probably as a result of the dealloying of Au/Ag alloy solid particles by reacting with the excess $HAuCl_4$. Such dual-color nanoparticles (i.e., with one extinction peak located in the green region and another in the red or NIR region) with tunable positions provide an optical feature similar to that of gold or silver nanorods, which are also characterized by two SPR peaks.[2b,c] In the case of Au nanorods, the peak originating from the longitudinal SPR mode can be swept from the red to NIR range with an increase of aspect ratio; the other peak attributed to the transverse mode is often located around 500 nm. Different from gold nanorods, the nanorattles are isotropic in three dimensions and are more compact in size (can be made as small as 50 nm in diameter).

Multiple-Walled Nanoshells of Metal Alloys. The solid core inside each nanorattle could also be replaced with a hollow nanoparticle to form nanoshells having multiple concentric walls (or nanoscale Matrioshka). As shown in the schematic illustration (Figure 4A), the Au/Ag alloy hollow nanoparticle could be prepared using the galvanic replacement reaction between solid Ag nanoparticle and $HAuCl_4$ (step I).[20] The surface of the resultant Au/Ag alloy nanoshell was then coated with a conformal, thin layer of pure Ag via an electroless plating process (step II). When the replacement reaction was repeated one more time, a new Au/Ag alloy nanoshell with slightly wider dimension would be formed, and a double-walled Au/Ag nanoshell was finally obtained (step III). Concentric nanoshells having more than two Au/Ag alloy walls could also be readily prepared by repeating step II and step III.

Figure 4B shows a typical TEM image of single-walled Au/Ag alloy nanoshells that were synthesized by reacting silver nanoparticles of ∼75 nm in mean diameter with $HAuCl_4$ solution. This image clearly indicates the formation of a void in the middle of each particle and the wall thickness of each shell was relatively uniform. EDX analysis on individual nanoshells indicated that they were composed of a Au and Ag

(28) (a) Yin, Y.; Li, Z.-Y.; Zhong, Z.; Gates, B.; Xia, Y.; Venkateswaran, S. *J. Mater. Chem.* **2002**, *12*, 522. (b) Mulvaney, P. *Langmuir* **1996**, *12*, 788.

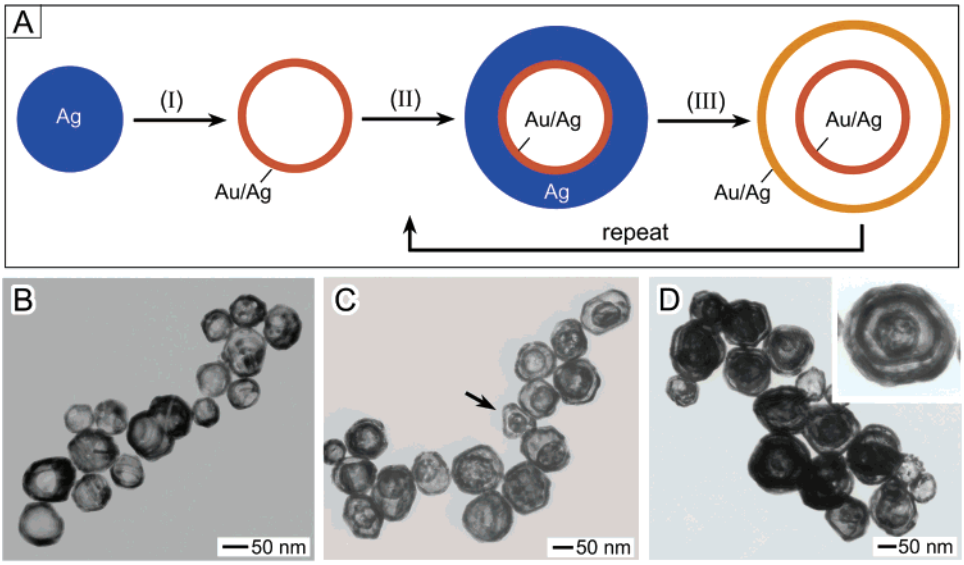

Figure 4. (A) Schematic procedure for fabricating multiple-walled nanoshells (Matrioshka) composed of Au/Ag alloys: (I, III) galvanic replacement reaction between Ag and $HAuCl_4$ and alloying between Ag and Au; (II) electroless deposition of pure silver on the surface of the Au/Ag alloy shell. The inner and outer Au/Ag shells may differ in elemental composition. (B−D) TEM images of three typical examples of Au/Ag alloy nanoshells that contained single (B), double (C), and triple (D) walls, respectively.

alloy.[20] The surfaces of these Au/Ag alloy nanoshells could then be directly coated with conformal shells of pure silver through the electroless plating process. The thickness of this new silver layer could be controlled by varying the concentration of $AgNO_3$ solution used for plating. After the replacement reaction was repeated, these silver-coated nanoshells were transformed into double-walled nanoshells (see Figure 4C for a typical TEM image), with each wall being composed of a Au/Ag alloy (probably with different compositions). Again, the spacing between outer and inner alloy shells was mainly determined by the thickness of silver coated in the electroless plating process. Note that the outer diameter of double-walled nanoshells had been increased to ~130 nm due to the formation of the outer shells. The size further increased as the number of shells was increased by repeating the two steps that involved silver coating and galvanic replacement reaction, respectively. As shown in Figure 4D, the mean outer diameter of the Au/Ag alloy nanoshells was increased to ~180 nm when a third shell was added. The inset clearly indicated that each particle was composed of three concentric shells.

Preservation of Shape in the Process of Electroless Plating and Galvanic Replacement Reaction. With the use of silver nanostructures having well-defined shapes, we have extensively studied the details associated with the galvanic replacement reaction between silver and aqueous $HAuCl_4$ solution.[20a] Electron diffraction and imaging studies clearly indicated that gold atoms resulting from the replacement reaction tended to nucleate and grow epitaxially on the surface of each single crystalline template of silver and thus to generate a Au/Ag alloy nanostructure with its morphology complementary to that of silver template. In the present work, we found that the double-walled nanoshell may exhibit distinctive morphologies for its two shells. For example, the particle indicated by an arrow in Figure 4C is composed of a spherical inner shell and triangular outer shell. It is believed that this remarkable difference in morphology was mainly caused by electroless plating of silver, in which the silver coating may not have epitaxially grown on the surface of the inner Au/Ag shell.

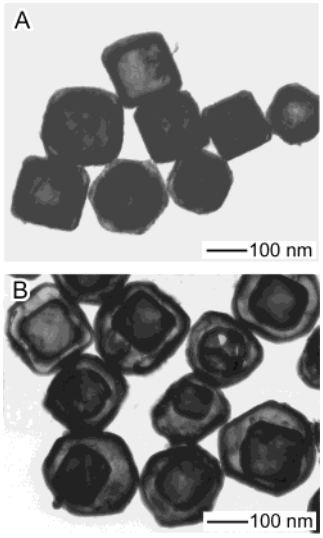

Figure 5. TEM images of double-walled, Au/Ag alloy nanoshells that were prepared with silver nanocubes as the initial template. Here, the spacing between the inner and outer shells was varied by controlling the thickness of the silver layer electrolessly deposited from $AgNO_3$ solutions of (A) 0.5 and (B) 1.3 mM in concentration.

We also studied the morphological relationship between the two shells of double-walled nanoshells derived from silver nanocube template. As the entire surface of each nanocube was bounded mainly by {100} facets, this template served as a better system to study morphological evolution and variation. Figure 5 shows the TEM images of two such samples of double-walled nanoshells with different spacings between the inner and outer shells. When the spacing was small (Figure 5A), the two shells of each particle exhibited the same cubic morphology. As the spacing between inner and outer shells was increased by increasing the thickness of the electroless plated silver layer (Figure 5B), the outer shells of most double-walled structures were characterized by shapes other than the cubic one. This dependence of shape on the spacing between shells reflects the variation in morphology for the silver coating. In general, a thinner deposition of silver tended to grow epitaxially on the

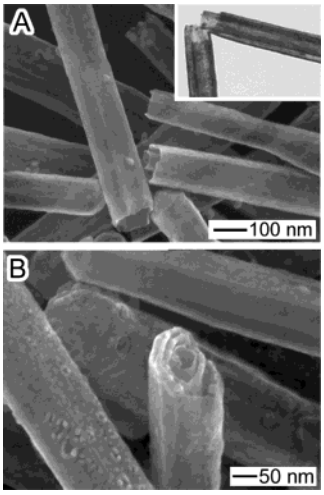

Figure 6. SEM images of metal nanotubes that were characterized by two (A) and three (B) coaxial walls, respectively. Each wall was composed of a Au/Ag alloy that might be slightly different in elemental composition. The inset shows a typical TEM image of two double-walled nanotubes.

surface of a Au/Ag nanoshell without assuming a shape different from that of the template. In comparison, a difference in growth rates for silver along various crystallographic directions usually led to the formation of a distorted shape once the thickness of silver coating had reached a critical value. This observation is consistent with the aforementioned result obtained for the preparation of Ag@Au core/shell colloids. In that case, thin gold layers grew epitaxially on the surfaces of silver seeds to form Ag@Au core/shell nanoparticles with a morphology similar to that of the silver template, although the silver layer deposited on gold nanoparticles did not necessarily have the facets of the original gold nucleus.[29] These studies demonstrate that we can control the morphology of the multiple-walled, concentric nanoshells by paying attention to the thickness of silver deposited via electroless plating.

Multiple-Walled Nanotubes Made of Metal Alloys. The unique combination of galvanic replacement reaction and electroless deposition of silver has also been extended to prepare nanotubes with multiple walls by using silver nanowire as templates. Figure 6A shows an SEM image of double-walled nanotubes consisting of Au/Ag alloy after they had been subjected to strong sonication (Sonics Vibracell, 30% power) for 1 h.[21] The broken tubes clearly show that each tube was composed of two coaxial sheaths characterized by a pentagonal cross section similar to that of the silver template. The inset shows a TEM image taken from the same sample, indicating that both inner and outer tubes along the longitudinal axis were hollow and uniform in dimension. Although the cross sections of both inner and outer walls of each double-walled tube were characterized by a pentagonal profile, the diameter of the outer tube along the longitudinal axis was not uniform in some cases. This nonuniformity could be ascribed to the fact that the deposition of silver sheaths on the Au/Ag nanotube might occur with different rates at different locations across the surface of a tube. Coaxial nanotubes with more than two walls could also be prepared by repeating the steps that involved silver plating and galvanic replacement reaction. For example, Figure 6B shows a typical SEM image of nanotubes composed of three coaxial, Au/Ag alloy walls. As a result of sonication, one of the tubes was fractured to clearly expose its triple-walled cross section.

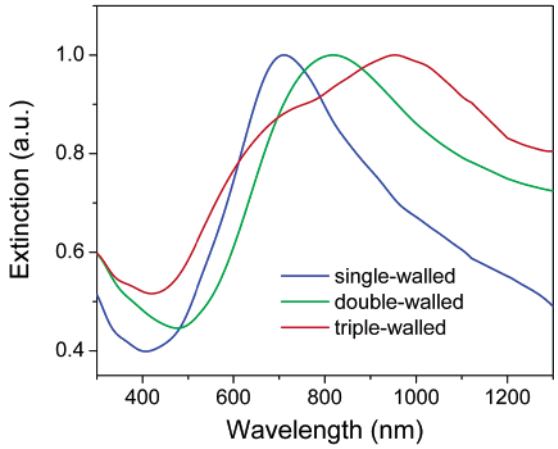

Figure 7. UV−vis−NIR extinction spectra of aqueous dispersions containing single-, double-, and triple-walled nanotubes composed of Au/Ag alloy. The spectra are normalized against their peak intensities.

The multiple-walled nanotubes made of Au/Ag alloy exhibited distinctive SPR features different from those of conventional Au/Ag alloyed nanoparticles. Figure 7 compares the UV−visible−NIR extinction spectra of Au/Ag nanotubes that contained one, two, and three sheaths of approximately the same elemental composition and wall thickness. For the single-walled nanotubes, the major SPR extinction peak was centered at 710 nm. This peak was red-shifted to 815 and 952 nm as the number of concentric walls increased to two and three. In the case of multiple-walled nanotubes suspended in a liquid medium (e.g., water), it was believed that the interaction (i.e., plasmonic coupling) between walls could be ignored because these walls were separated by more than 10 nm as the void between them filled with dielectric liquid.[30] Different from the nanorattle structures shown in Figure 2B, the inner tube seemed to be positioned in the center of each concentric tube due to the reduced magnitude for Brownian motion. As a result, the extinction peak should be the transverse SPR mode corresponding to the outmost tube. Because each wall of a multiple-walled nanotube had approximately the same elemental composition and thickness, the red-shift observed for the SPR peak is primarily caused by the increase in lateral dimension for the outmost tube.[8b]

Hollow Nanostructures Consisting of Hybrid, Multiple Walls. As we have demonstrated in previous studies, silver nanoparticles could also serve as a sacrificial template to generate nanoshells made of metals other than Au/Ag alloys by reacting with appropriate precursor salts. For instance, it is possible to generate nanoshells consisting of Pd/Ag alloys by reacting silver nanoparticles with palladium salts because the standard redox potential of the Pd^{2+}/Pd pair (0.83 V versus the standard hydrogen electrode, or SHE) is higher than that of the Ag^{+}/Ag pair (0.80 V versus SHE).[31] On the basis of this notion, we have successfully fabricated double-walled nanoshells with hybrid compositions (i.e., the outer and inner shells composed of Pd/Ag and Au/Ag alloys, respectively) by reacting Ag-coated

(29) Hodak, J. H.; Henglein, A.; Giersig, M.; Hartland, G. V. *J. Phys. Chem. B* **2000**, *104*, 11708.

(30) Schierhorn, M.; Liz-Marzán, L. M. *Nano Lett.* **2002**, *2*, 13.

(31) Sun, Y.; Tao, Z.; Chen, J.; Herricks, T.; Xia, Y. *J. Am. Chem. Soc.* **2004**, *126*, 5940.

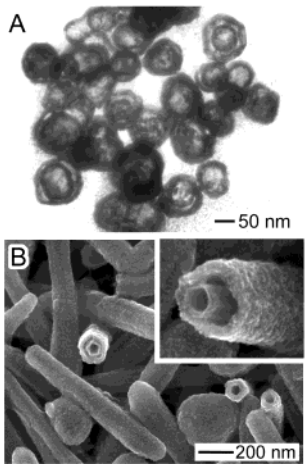

Figure 8. Typical TEM image of double-walled nanoshells (A) and nanotubes (B) with the constituent material being a Au/Ag alloy and a Pd/Ag alloy for the inner and outer layers, respectively.

Au/Ag alloy nanoshells with an aqueous $Pd(NO_3)_2$ solution. Figure 8A gives a TEM image of such double-walled nanoshells, indicating that the surfaces of Pd/Ag alloy shells were rougher than those of Au/Ag alloy shells. A closer examination by TEM revealed that the outer Pd/Ag alloy nanoshells were polycrystalline and were constructed from small particles with grain sizes in the range of 2−10 nm. The poor crystallinity of Pd/Ag alloy shells might be related to the lattice mismatch between Pd and Ag (∼4.8%), which may prevent Pd atoms from growing epitaxially on the surface of silver.

By reacting Ag-coated, single-walled Au/Ag nanotubes with $Pd(NO_3)_2$ in the second round of replacement reaction, double-walled nanotubes with hybrid compositions were also fabricated (see Figure 8B for an SEM image). In this sample, the outer and inner walls of each tube were constructed from Pd/Ag and Au/Ag alloys, respectively. The inset gives the SEM image of an individual, broken nanotube with slightly higher magnification, clearly showing that the side surfaces of Pd/Ag alloy tube (i.e., the outer wall) were rougher than those of Au/Ag alloy tube (i.e., the inner wall). Similar to the nanoshells shown in Figure 8A, the surface roughness could also be attributed to the polycrystallinity of the Pd/Ag sheath. The hollow nanostructures consisting of polycrystalline Pd/Ag may exhibit superior performance in areas such as catalysis and gas storage because a polycrystalline material generally has a higher surface area than its single crystalline counterparts.[31,32] These hollow nanostructures containing hybrid, multiple walls may also find use in applications that require a combination of different functions.

4. Conclusion

The galvanic replacement reaction between Ag and $HAuCl_4$ and the electroless deposition of silver have been combined to provide a unique route to a number of new, complex core/shell metal nanostructures. For example, nanorattles containing potentially movable Au/Ag alloy cores have been synthesized by templating against Au/Ag alloy colloids with relatively high percentages of gold; nanoshells/nanotubes consisting of multiple walls (nanoscale Matrioshka) of Au/Ag alloys have been prepared by starting with silver nanoparticles/nanowires as the initial template. In addition, double-walled nanoshells characterized by hybrid compositions have been fabricated by using different salts, $HAuCl_4$ and $Pd(NO_3)_2$, in different steps of the galvanic replacement reaction. In general, the composition and configuration of these core/shell nanostructures were mainly determined by the starting templates and the salt precursors taking part in the replacement reaction. It is believed that this technique can be readily extended to produce more complex core/shell nanostructures by incorporating more metals (or alloys) into the synthetic scheme. The nanostructures described here represent a class of largely unexplored nanomaterials that may exhibit plasmonic and catalytic properties different from those of solid or conventional core/shell nanoparticles made of gold and silver.

The procedures described in this article have not been optimized by all means. In a typical run of synthesis (as shown in Figure 2), the specific core/shell nanostructures could be obtained at a concentration of $\sim 1.7 \times 10^{11}$/mL and with a yield of ∼95%. We note that this concentration is as high as those of commercial samples of gold colloids provided by Ted Pella (Redding, CA), where the typical concentrations are in the range of 3.6×10^{8}/mL to 4.5×10^{10}/mL for particles with diameters between 250 and 50 nm. In general, the highest particle concentration that we can work with for a replacement reaction is limited by the solubility of AgCl precipitate.[20a] We need to keep AgCl soluble at 100 °C to obtain well-defined Ag/Au alloy nanoshells. By taking the solubility product constant (K_{sp}) of AgCl as 1.2×10^{-6} at 100 °C, the highest concentration for the Ag-coated Au/Ag nanoparticles (shown in Figure 2A) is estimated to be around 3×10^{12}/mL. For the core/shell structures with multiple walls, the number of defects increased as the number of walls increased due to the accumulation and propagation of defects. It might be possible to solve this problem by purifying the product at each step of the synthesis. These new core/shell nanostructures of metals and alloys are expected to find use in a range of applications. For example, computational studies suggested that Au/Ag alloy nanotubes with pentagonal cross sections might serve as excellent substrates for the surface-enhanced Raman spectroscopic (SERS) detection of molecular species with ultrasensitivity in the spectral region from red to near-infrared, which happens to be a transparent window for biological samples.[33]

Acknowledgment. This work has been supported in part by a DARPA-DURINT subcontract from Harvard University, a Career Award from NSF (DMR-9983893), and a research fellowship from the David and Lucile Packard Foundation. Y.X. is a Camille Dreyfus Teacher Scholar and an Alfred P. Sloan Research Fellow. We thank Prof. D. Gamelin for allowing us to use the UV−vis−NIR spectrometer in his research group.

Supporting Information Available: TEM images, table of percentage of cores stuck to a particular side of the shell, and plot of the extinction coefficient. This material is available free of charge via the Internet at http://pubs.acs.org.

JA048789R

(32) Kim, S.-W.; Kim, M.; Lee, W. Y.; Hyeon, T. *J. Am. Chem. Soc.* **2002**, *124*, 7642.

(33) Kottmann, J. P.; Martin, O. J. F.; Smith, D. R.; Schultz, S. *Phys. Rev. B* **2001**, *64*, 235402.